ESCUELA DE CONSTRUCCIÓN CIVIL
FACULTAD DE INGENIERÍA

Revista de la Construcción
Journal of Construction

Research Article

Numerical investigation of the behavior of reinforced concrete beams produced with self-compacting concrete

Salih Cengiz [1], Abdulkadir Solak [2], *, Alptuğ Ünal [3], Mehmet Kamanlı [4]

[1] Department of Construction, Vocational School of Technical Sciences, Konya Technical University, Konya (Türkiye); email: scengiz@ktun.edu.tr
[2] Department of Civil Engineering, Faculty of Engineering and Natural Sciences, Konya Technical University, Konya (Türkiye); email: abdulkadirsolak@ktun.edu.tr
[3] Department of Civil Engineering, Faculty of Engineering and Natural Sciences, Konya Technical University, Konya (Türkiye); email: aunal@ktun.edu.tr
[4] Department of Civil Engineering, Faculty of Engineering and Natural Sciences, Konya Technical University, Konya (Türkiye); email: mkamanli@ktun.edu.tr
*Correspondence: abdulkadirsolak@ktun.edu.tr (A. Solak)

Received: 14.07.23; **Accepted:** 11.03.24; **Published:** 31.08.24

Citation: Salih, C., Abdulkadir, S., Ünal, A. and Kamanlı, M. (2024). Numerical investigation of behavior of reinforced concrete produced with self-compacting concrete beams. Revista de la Construcción. Journal of Construction, 23(2), 271-295. https://doi.org/10.7764/RDLC.23.2.271

Abstract: In this study, 1/2 scaled 16 reinforced concrete beams were compared in terms of concrete type, concrete strength, and stirrup spacing. The variables of this study consist of self-compacting concrete and normal concrete as concrete type, C30 and C60 as concrete strength, and without stirrup, 20 cm, 10 cm and 5 cm spacing as stirrup spacing. All elements were tested with 4-point bending mechanism. The stiffness, ductility, load bearing capacity and energy consumption capacity values of the beams were obtained from the load-displacement curves acquired from the experimental study and the elements were compared over them, and the damages of the beams during the experiments were interpreted. In addition to the experimental study, the numerical analyzes of the beams were conducted with the finite element analysis software. Experimental study results were validated by finite element analysis. When all the results were examined, it was concluded that although the initial stiffness of SCC (self-compacting concrete) was less than NC (normal concrete), the ductility of SCC was higher than that of NC, especially in high strength concretes.

Keywords: reinforced concrete beam, behavior, numerical analysis, stirrup spacing, self-compacting concrete.

1. Introduction

Reinforced concrete structures that have shaped our world for more than 150 years are indispensable to the construction sector with their economic and mechanical advantages. Although more than a century and a half have passed since its invention, it is still being studied and many weaknesses are trying to be developed. In order to improve the weaknesses of concrete, special concrete has been invented. Self-compacting concrete (SCC), which emerged in Japan in the 1980s, was found due to difficulties in placement and compacting in normal concrete (NC). (Okamura, 1997; Okamura and Ouchi, 1999).

SCCs are defined as the concrete having the ability to settle in the mold and pass through the rebars without being decomposed with their own weight without the need for any external effects (vibration, rodding, etc.). The SCC must have a high fluency. At the same time, decomposition and water desorption (bleeding) events should not occur. While high fluidity is achieved by super plasticizers, it is necessary to increase the amount of fine material or use viscosity-increasing additives to avoid decomposition. (Topçu et al., 2008). Historically, more than a century of time between NC and SCC suggests that many more studies are needed to be conducted on the SCC. Therefore, more comparative studies are needed to definitively determine whether SCC should categorically replace NC.

1.1. Literature review

As a result of extensive literature research, it has seen that many experimental and theoretical researches about SCC have been done (Ahmad et al., 2017; Akinpelu et al., 2017; Alexandra et al., 2018; Altın et al., 2006; Alyousif et al., 2015; Aydın and Bayrak, 2016; Benaicha et al., 2019; El Zareef and El Madawy, 2018; Fiol et al., 2018; Hemzah et al., 2020; Jindal et al., 2019; Kamal et al., 2018; Khan and Ayub, 2020; Mahmod et al., 2018; Niewiadomski et al., 2018; Pająk, 2016; Pająk and Ponikiewski, 2017; Shatarat et al., 2018; Akça et al., 2023; Alabdulkarim et al., 2024). It is one of these to discover the flexural strength properties of beam specimens produced by SCC. However, the researchers produced specimens by using pure concrete instead of a reinforced concrete system in their work. This does not help to fully understand the effect of physical and mechanical differences of SCC on reinforced concrete systems used in buildings. In this study, it will be investigated how reinforced concrete beams with different stirrup spacing and concrete strength produced by SCC will behave differently from the same properties of reinforced concrete beams produced with NC.

Beams, which are one of the supporting elements in reinforced concrete structures, are the structural elements that transfer the loads onto the columns. It is very important for building safety to investigate and develop the behavior of these elements under various loads. There are many studies in the literature on reinforced concrete beams (Abd et al., 2023; Alam and Hussein, 2017; Alhadid and Youssef, 2017; Ebead, 2015; El-Sayed, 2017; Jiang et al., 2018; Kaltakci and Kamanli, 2001; Kamanlı, 1999; Kodur et al., 2018; Mohammed, 2017; Özkılıç et al., 2023; Pawłowski and Szumigała, 2015; Qeshta et al., 2015; Yang et al., 2017; Yousef et al., 2018). With these researches, the behavior of reinforced concrete beams under various loads and conditions was tried to be determined.

It is known that stirrup is very important in terms of shear safety in reinforced concrete beams. Studies on the effect of stirrup spacing on the behavior of reinforced concrete beams are not much. In these studies, the effect of stirrup on reinforced concrete beam behavior was investigated and important findings have been obtained (Cengiz, 2019; Cladera and Mari, 2005; Kamanli and Unal, 2018; Rahal and Alrefaei, 2018; Sin et al., 2011; Unal et al., 2018; Yuan and Wang, 2019).

Cengiz et al., 2020, experimentally tested reinforced concrete beams produced with SC and NC concretes. The strength of the concretes is 30 MPa and 60 MPa. The other parameter of the study is the stirrup spacing. The stirrup spacings they used to be 0, 20, 10 and 5 cm. The researchers chose the beam dimensions as 25 cm height and 12.5 cm width. In the results, only load-displacement graphs were given. In this study, the tests of beams produced with both C30 and C60 strength concrete were carried out. In addition to the load-displacement graphics, rigidity, energy consumption, slope-angle graphics are also given in the test results. Experimental study was supported by numerical analysis.

In the light of all these evaluations, an experimental study was carried out to investigate the flexural behavior of reinforced concrete beams produced with SCC. In this study, 1/2 geometrically scaled 16 reinforced concrete beam specimens were tested under monotonic loading with 4-point bending mechanism. Concrete type, concrete strength and stirrup spacing are the variables of this study. As a result of the study, load-displacement curves, stiffness graphs and energy consumption graphs of the beams were drawn and the results were evaluated comparatively. Furthermore, the cracks were drawn during the experimental study and the effects of the cracks on the beam behavior were examined. In addition to the experimental study, the numerical analyzes of the beams were conducted with the finite element analysis software (Ansys, Release 19.2). Experimental study results were validated by finite element analysis. According to the results, it was seen that the reinforced concrete beams produced with SCC consumed more energy and displaced than those produced with NC.

When the literature is examined, most of the studies with SCC are done without using reinforcement. However, reinforcement in the concrete must be used in the buildings. In this study, reinforcement was used in beams produced with SCC. With this study, the effect of compressive strength and stirrup spacing changes on reinforced concrete beams produced with SCC were investigated. In addition, SCC and NC beams were compared in terms of load bearing capacity, ductility, stiffness, energy consumption and damage during the test.

This study was carried out to investigate the difference in the behavior of NC and SCC with the same strength in reinforced concrete beams under different transverse reinforcement density. In the numerical analysis, a more realistic modeling was performed by using different material properties for SCC and NC. In this study, firstly numerical modeling was performed based on the experimental results, then the results obtained from the numerical analysis were compared with the experimental results and finally the behavioral properties obtained in the conclusion section were discussed.

2. Materials and methods

In this study, the bending behavior of reinforced concrete beams produced with SCC and NC was numerically investigated. Within the scope of the numerical study, a total of 16 reinforced concrete beams with 1/2 scale were tested under 4-point bending (Figure 1). Concrete type, concrete strength and stirrup spacing are the variables of this study. SCC and NC were chosen as concrete type, and C30 (cylinder compressive strength approximately 30 MPa) and C60 (cylinder compressive strength approximately 60 MPa) were selected as concrete strength. Reinforced concrete beams are designed with 5 cm, 10 cm, 20 cm stirrup spacings and without stirrups (Figure 4). For this reason, the beams are designed as C30 and C60 concrete class. Sample dimensions are 125x250x2500 mm. In order for the beams to exhibit bending behavior, the ratio of shear span to effective depth (a/d) was chosen as 3.33. The properties of the test samples are shown in Table 1. In the test elements, N and S represent the type of concrete, 0-20-10-5 represent stirrup spacing, as well C30 and C60 represent concrete compressive strength.

Table 1. The properties of specimens.

Specimen	Concrete type	Compressive strength	Stirrup spacing
N-C30-0	NC	30 MPa	-
N-C30-20	NC	30 MPa	200 mm
N-C30-10	NC	30 MPa	100 mm
N-C30-5	NC	30 MPa	50 mm
N-C60-0	NC	60 MPa	-
N-C60-20	NC	60 MPa	200 mm
N-C60-10	NC	60 MPa	100 mm
N-C60-5	NC	60 MPa	50 mm
S-C30-0	SCC	30 MPa	-
S-C30-20	SCC	30 MPa	200 mm
S-C30-10	SCC	30 MPa	100 mm
S-C30-5	SCC	30 MPa	50 mm
S-C60-0	SCC	60 MPa	-
S-C60-20	SCC	60 MPa	200 mm
S-C60-10	SCC	60 MPa	100 mm
S-C60-5	SCC	60 MPa	50 mm

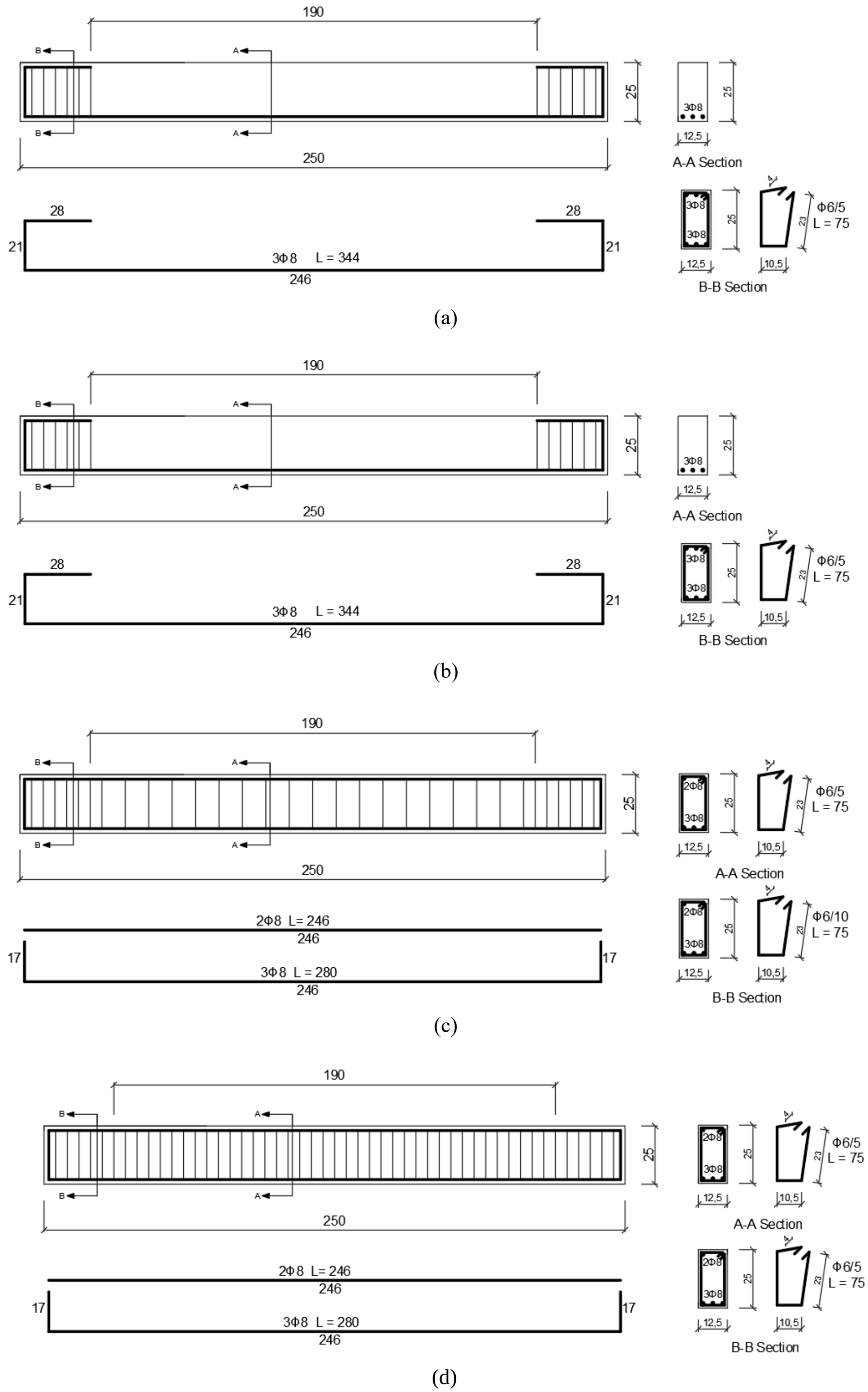

Figure 1. Reinforcement rebar detailing (a) without stirrup, (b) 200 mm, (c) 100 mm, (d) 50 mm.

2.1. Test setup and loading protocol

A total of 16 specimens were analyzed under monotonic loading using ANSYS Workbench 19.2. The support and loading conditions in the analysis model used in the numerical study were obtained from the experimental setup carried out by the authors at Konya Technical University, Department of Civil Engineering, Earthquake Research Laboratory. In the model, bearings and loading plates are designed rigid (Figure 2).

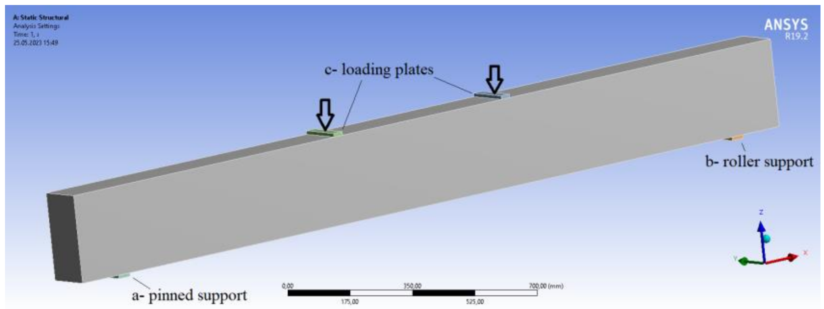

Figure 2. Conditions of analysis.

The displacement capacity of the specimens was also determined from the data obtained from the experimental study. The loading protocol was designed according to the displacement capacity of the specimens (Figure 3). During the analysis, displacement-controlled loading method was applied to the specimens. As a result of the analysis, the load values corresponding to each displacement value were determined. Load-midpoint displacement graphs were plotted with the help of the obtained data.

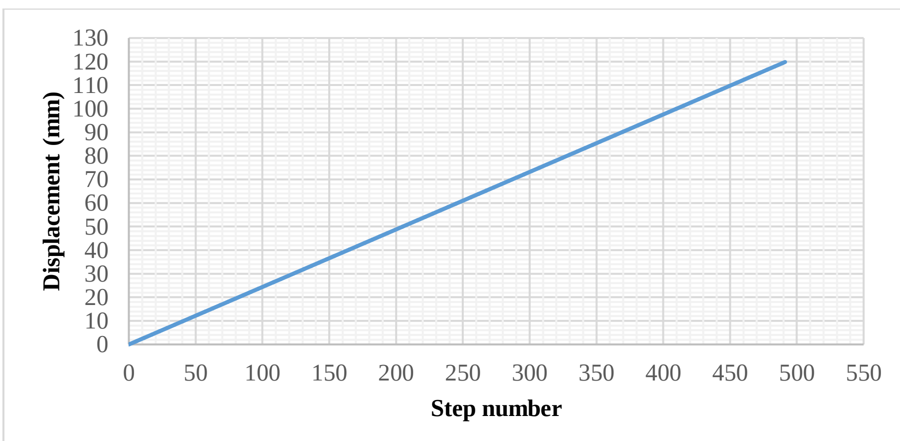

Figure 3. Loading protocol.

2.2. Material properties

The SOLID65 element was used to model the concrete. This element has eight nodes with three degrees of freedom at each node - node translations in x, y and z directions. This element is capable of plastic deformation in concrete applications, cracking in three orthogonal directions and crushing in compression (Figure 4).

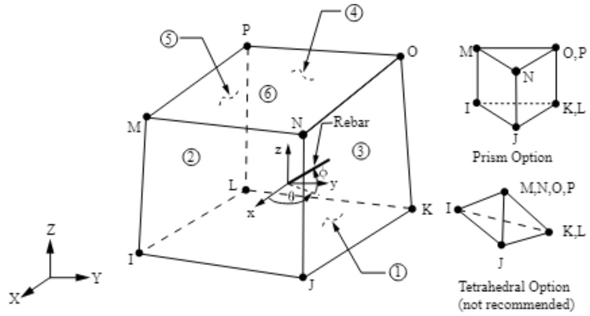

Figure 4. SOLID65 geometry (ANSYS, 2018).

The following equation which proposed by Hognestad have used for computing the multilinear isotropic stress–strain curve for the concrete (Hognestad, 1951), where σ_c and ε_c are concrete stress and concrete strain in general, respectively; f_c is the concrete compressive strength; ε_{co} is the concrete strain at peak stress. The tensile strength of concrete was determined by 4-point bending test in order to be appropriate for the loading condition to be applied in the experimental study and numerical study.

$$\sigma_c = f_c \left[\frac{2\varepsilon_c}{\varepsilon_{co}} - \left(\frac{\varepsilon_c}{\varepsilon_{co}} \right)^2 \right] \qquad (1)$$

The stress-strain values determined according to the Hognestad model for NC are shown in Table 2. The modulus of elasticity was calculated using the initial slope of the σ-ε graph obtained from the values. The Modulus of Elasticity for SCC was used by decreasing it by 15% (Ünal et al., 2023). Because it was determined that the rigidity values of the reinforced concrete beam samples tested in this study up to tensile breakage decreased at this rate. The Poisson ratio is taken as 0.2 for both concrete samples. Since the fine aggregate ratio is high in the self-compacting concrete samples, the interfacial area has increased. Therefore, the tensile strength of concrete increases compared to normal concrete. In addition, the concrete tensile strength of SCC samples was increased by 7.5% as the aggregates in the concrete mixture were distributed more homogeneously than normal concrete (Ahmad et al., 2017) (Table 3). 2-node linear displacement truss element LINK180 is adopted for the beam longitudinal reinforcement and stirrups. The element is a uniaxial tension-compression element with three degrees of freedom at each node: translations in the nodal x, y, and z directions (Figure 5).

Table 2. Multilinear isotropic stress-strain values.

Concrete type	Strain (ε)				
	0.001025	0.0015	0.002	0.0025	0.003
N-C30	25.40	31.37	33.32	31.24	25.00
N-C60	45.17	55.55	59.26	55.25	44.45
S-C30	25.65	31.54	33.65	31.54	25.24
S-C60	48.62	59.79	63.78	59.79	47.84

Table 3. Mechanical specifications of concrete.

Element type	Concrete type	Ultimate compressive strength (f_c)	Elastic modulus (MPa)	Poisson's ratio	Ultimate tensile strength (f_{ct})
SOLID65	NC	33.32 MPa	24781.75	0.2	3.22 MPa
		59.26 MPa	44074.63		5.78 MPa
	SCC	33.65 MPa	21273.10		3.43 MPa
		63.78 MPa	40320.91		6.26 MPa

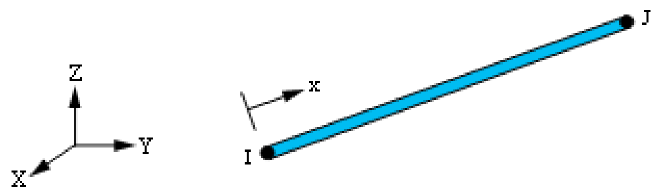

Figure 5. LINK180 geometry (2018).

The beams were designed according to Turkish Building Earthquake Code 2018 (TBEC, 2018). Stirrup spacings used according to the code are modelled as 0, 20, 10 and 5 cm. Beam dimensions were also designed as 50 cm height and 25 cm width to meet the minimum requirements in the code. However, since the beam dimensions were modelled in 1/2 scale in the experimental study, they were scaled to 25 cm height and 12.5 cm width in the models. Therefore, 8 mm diameter longitudinal reinforcements and 6 mm diameter stirrups were used in the beams.

Table 4. Mechanical specifications of reinforcement.

Element type	Reinforcement	Yield strength re (MPa)	Tensile strength rm (MPa)	Rm/Re	Poisson's ratio	Elastic modulus (MPa)
LINK180	Ø6	337.33	483.4	1.43	0.3	208.210
	Ø8	318.93	428.3	1.34		204.183

2.3. FE Model numerical assessments

Since concrete is a complex construction material and concrete is regarded as a quasi-brittle material that behaves differently under tension and compression, many models have been proposed for numerical modelling of concrete. In this study, Willam-Warnke "Constitutive model for the triaxial behavior of concrete" was used for the crack model of concrete material (Willam, 1974). In the literature, this model has been used in experimental and numerical studies on simply supported beams under monotonic load since the experimental and numerical results are compatible (Hosseinimehrab et al., 2021; Ugur and Unal, 2022). Shear transfer coefficients was taken 0.3 for open crack, 1.0, for close crack. These coefficients are used to reduce the error rate when obtaining the load-displacement relationship derived by the finite element method. The mechanical behavior of reinforcement is assumed to be elastic bilinear under monotonic stress.

The reinforcement initially exhibits a linear elastic part, followed by a yield point, strain hardening and then fracture. The main inputs to include the steel material model are modulus of elasticity, tangent modulus and yield strength. The tangent modulus (k) is taken as 20000 MPa in the analysis. The constitutive models for steel and concrete under compression is given in Figure 6.

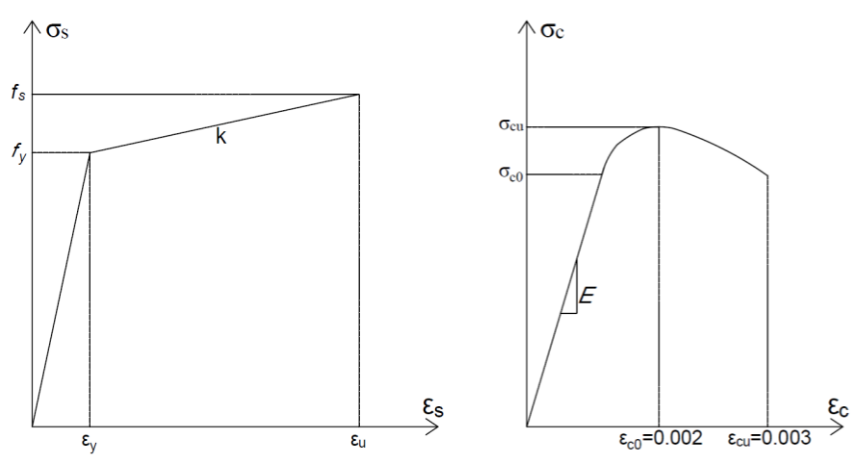

Figure 6. Constitutive model of (a) reinforcement, (b) concrete under compression.

Figure 7 shows the mesh of the beam specimen. The load and boundary conditions of the FE model were set to be the same as the beam in the experimental study. The a/d ratio of the samples was assumed to be 3.33. All displacements at one support of the beam are limited. Displacement along the x direction is allowed for the other support of the beam. Displacement loads equal to the experimental study are applied to the rigid loading plates on the beam. Before the numerical study, preliminary analyses were performed to verify the experimental study. In addition, the mesh dimensions and analysis properties were converged with the experimental study as a result of many preliminary analyses, and finite element and analysis properties were obtained by optimizing for all models. The nonlinear specimen models were analyzed under monotonic load.

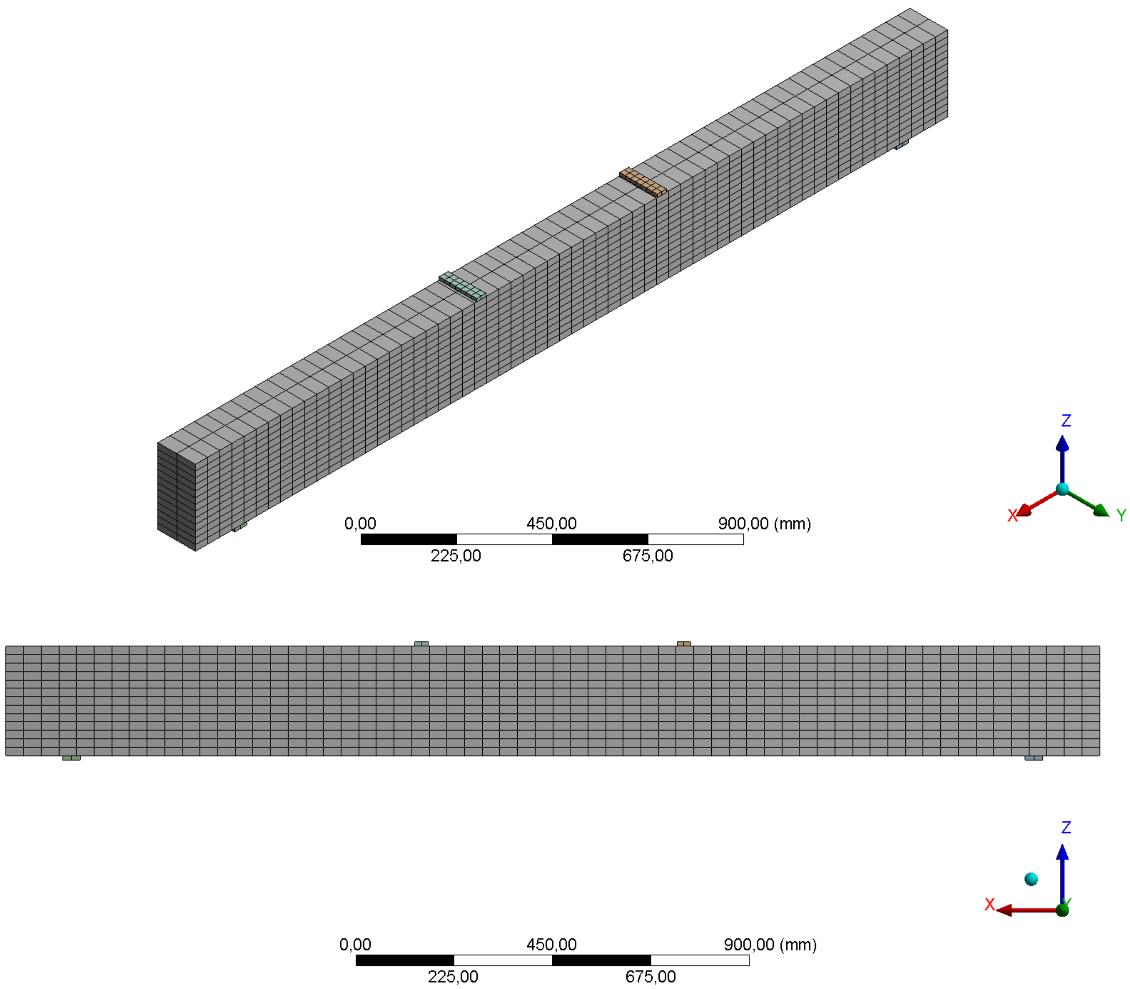

Figure 7. FE model of beams.

3. Results and analysis

This study investigated the behavior of NC and SCC in reinforced concrete beams. 16 reinforced concrete beams were designed at 1/2 scale and analyzed under 4-point bending. In all analyses carried out, the beams reached the yield point prior to failure. Stress concentrations in the flexural region occurred in all test specimens until yielding. In the specimens without stirrups, flexural behavior was observed up to any displacement value and shear behavior was observed after this value. S-C30-0, N-C30-0, N-C60-0 and S-C60-0 elements reached failure due to shear stresses after yielding. In other specimens, only flexural behavior was observed until failure.

The load-displacement curves obtained from the numerical analysis are shown in Figure 8. From the load-displacement curves of the specimens, the general beam behavior, failure modes, strengths, stiffness, ductility values and energy consumption capacities were determined and the results were evaluated. Load-displacement, angle of deflection and cumulative energy consumption curves were used to compare the specimens. The specimens tested for each configuration are shown in Table 5. The data obtained from all specimens are shown in Table 6.

Table 5. Specimen tested for each configuration.

Comparison	Specimens
Effect of stirrup spacing	A) N-C30-0, N-C30-20, N-C30-10, N-C30-5 B) S-C30-0, S-C30-20, S-C30-10, S-C30-5 C) N-C60-0, N-C60-20, N-C60-10, N-C60-5 D) S-C60-0, S-C60-20, S-C60-10, S-C60-5
Effect of concrete type	A) N-C60-0 and S-C60-0 B) N-C60-20 and S-C60-20 C) N-C60-10 and S-C60-10 D) N-C60-5 and S-C60-5
Effect of concrete strength	A) S-C30-0 and S-C60-0 B) S-C30-20 and S-C60-20 C) S-C30-10 and S-C60-10 D) S-C30-5 and S-C60-5

3.1. Effect of stirrup spacing

When the beam specimens designed with the same material properties and with different stirrup spacings were compared, it was found that the yield points of the beams with the same stirrup spacing were in the range of 40 - 45 kN. The yield strength of the NC beams is higher than the SCC beams. This is due to the amount of coarse aggregate in the concrete content. In fact, the proportion of coarse aggregate is higher in NC than in SCC.

The load-displacement graphs of the specimens for variation of stirrup spacing are shown in Figure 8. In general, an increase in stirrup spacing resulted in an increase in displacement. As the stirrup spacing increases, the failure mode of the members approaches shear failure. According to the graphs, N-C30-5 was the specimen with the highest load capacity, bearing a load of 51.6 kN. However, N-C30-5 fractured at a displacement range of approximately 90 mm due to a sudden and severe compressive fracture during loading, consuming less energy than the other specimens. Shear fracture occurred in all specimens without stirrups.

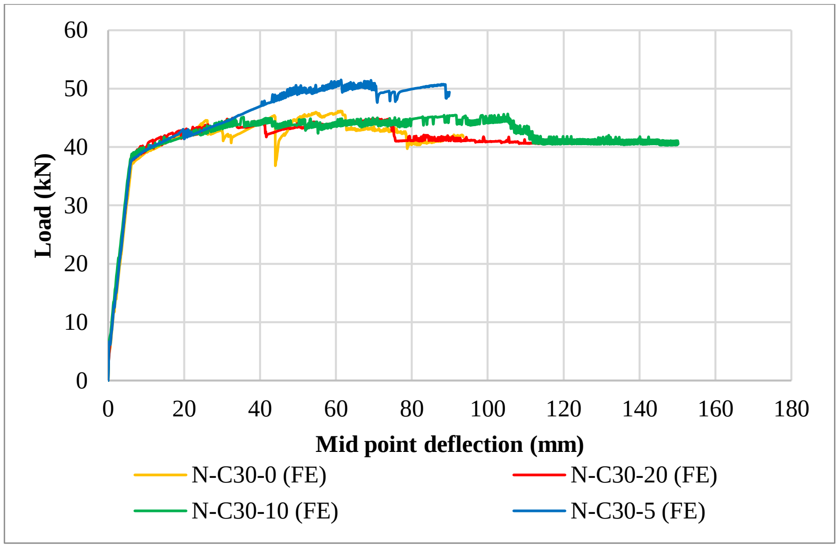
60
50
40
30
20
10
0
Load (kN)
0
20
40
60
80
100
120
140
160
180
Mid point deflection (mm)
N-C30-0 (FE)
N-C30-20 (FE)
N-C30-10 (FE)
N-C30-5 (FE)

(a)

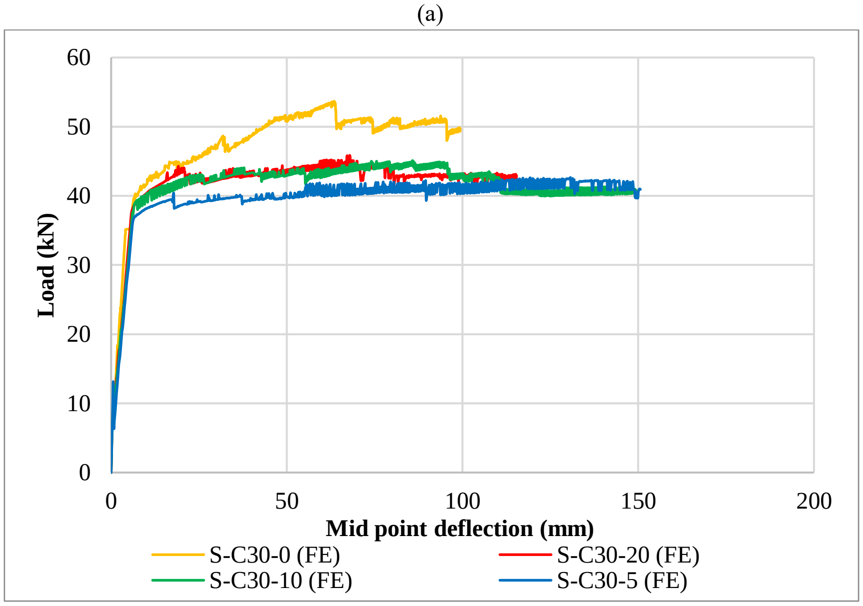
60
50
40
30
20
10
0
Load (kN)
0
50
100
150
200
Mid point deflection (mm)
S-C30-0 (FE)
S-C30-20 (FE)
S-C30-10 (FE)
S-C30-5 (FE)

(b)

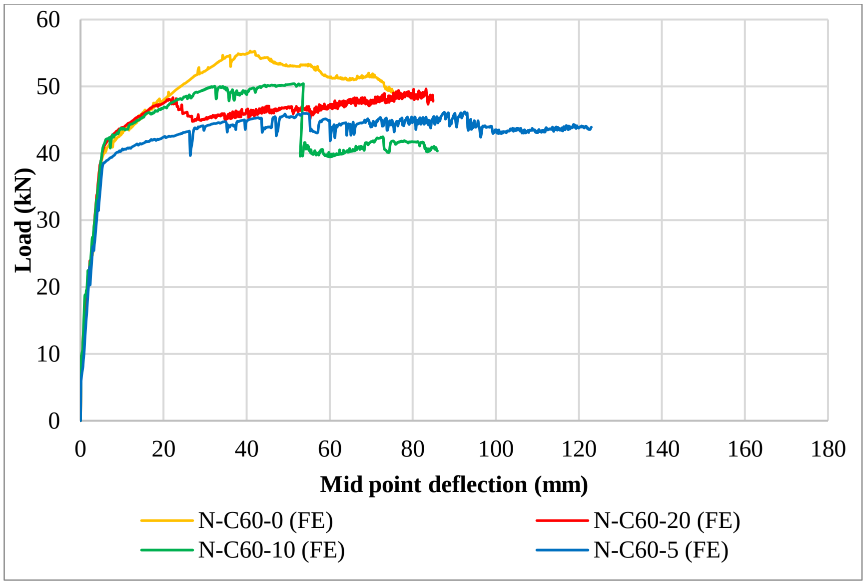

(c)

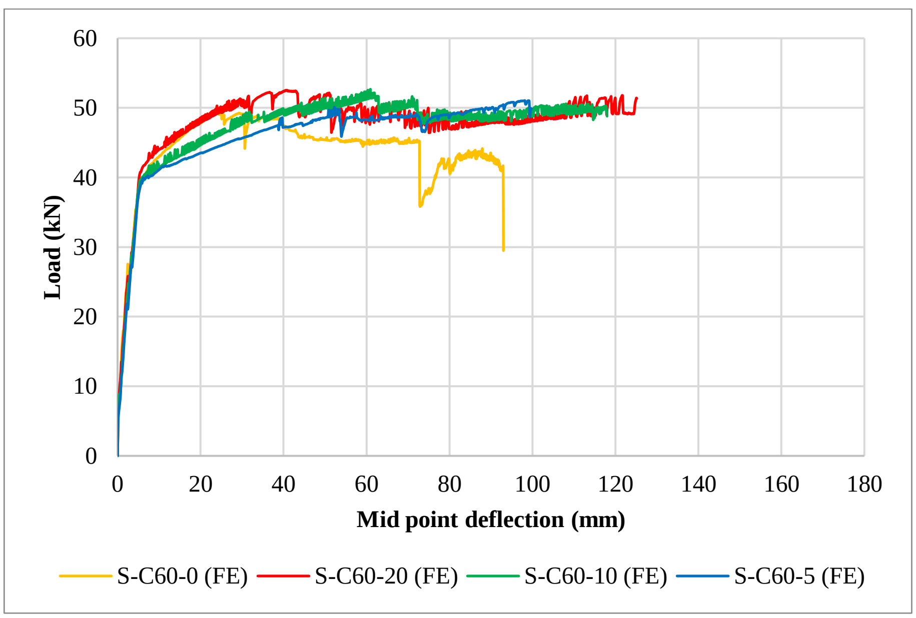

(d)

Figure 8. Load-displacement graphs for variation of stirrup spacing (a) N-C30, (b) S-C30, (c) N-C60, (d) S-C60.

The energy consumption graphs for variation of stirrup spacing are shown in Figure 9. N-C60 specimens, the beam with 10 cm stirrups consumed the most energy of all the other specimens. It can be seen that the energy consumption values of the low stirrup and no stirrup specimens are lower than the other specimens. The energy consumption of all specimens at the yield point is between 2.81 kN.m and 11.70 kNm. The specimen with the highest energy consumption is S-C30-5 and the specimen with the lowest energy consumption is N-C60-0.

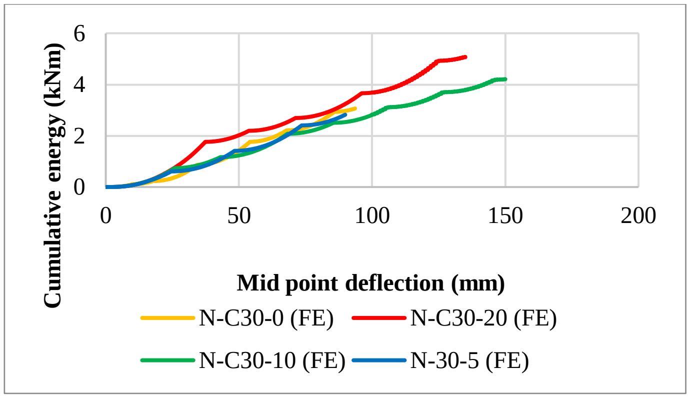
Cumulative energy (kNm)
6
4
2
0
0
50
100
150
200
Mid point deflection (mm)
N-C30-0 (FE)
N-C30-20 (FE)
N-C30-10 (FE)
N-30-5 (FE)

(a)

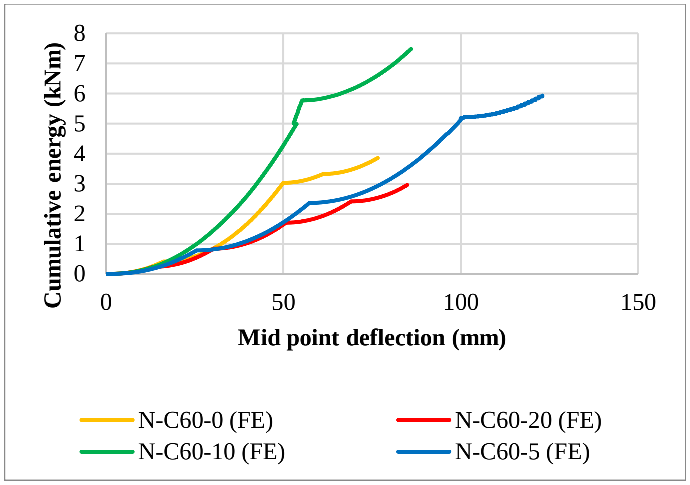
Cumulative energy (kNm)
8
7
6
5
4
3
2
1
0
0
50
100
150
Mid point deflection (mm)
N-C60-0 (FE)
N-C60-20 (FE)
N-C60-10 (FE)
N-C60-5 (FE)

(b)

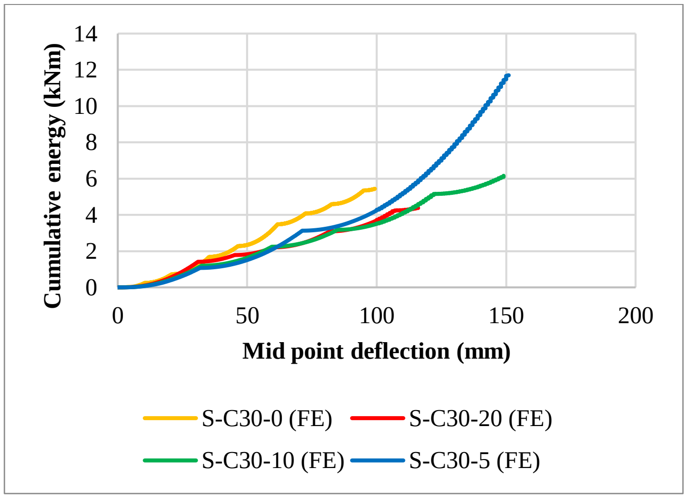
Cumulative energy (kNm)
14
12
10
8
6
4
2
0
0
50
100
150
200
Mid point deflection (mm)
S-C30-0 (FE)
S-C30-20 (FE)
S-C30-10 (FE)
S-C30-5 (FE)

(c)

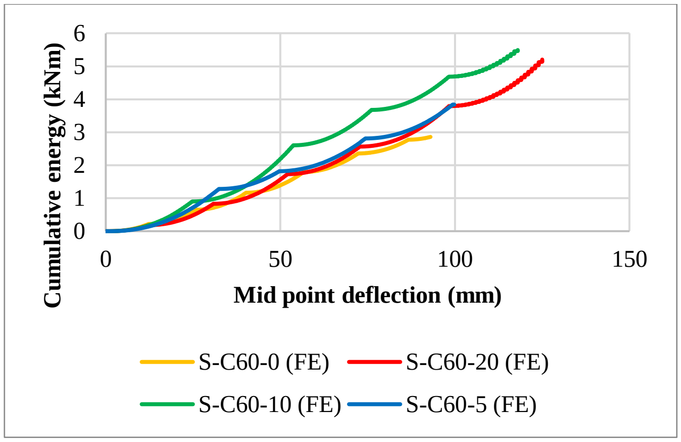

(d)

Figure 9. Energy consumption graphs for variation of stirrup spacing (a) N-C30, (b) S-C30, (c) N-C60, (d) S-C60.

3.2. Effect of concrete type

To investigate the effect of concrete type on the behavior of reinforced concrete beams, beams designed with a concrete strength of 60 MPa and with the same stirrup spacing were compared. Load-displacement graphs for the variation in concrete type are shown in Figure 10. When the graphs are examined, it can be seen that the load carrying capacity of the NC beams is 12.05% higher in the specimens with no stirrups, 7.77% higher in the RC beams with 20 cm stirrup spacing, 4.40% higher in the RC beams with 10 cm stirrup spacing and 8.84% higher in the RC beams with 5 cm stirrup spacing compared to SCC. On the other hand, with the exception of the beam with 5 cm stirrup spacing, SCC has a higher displacement value compared to NC than all other beams. This had a direct effect on the energy plots. The highest displacement value was calculated for S-C60-20 with a displacement value of 124.7 mm.

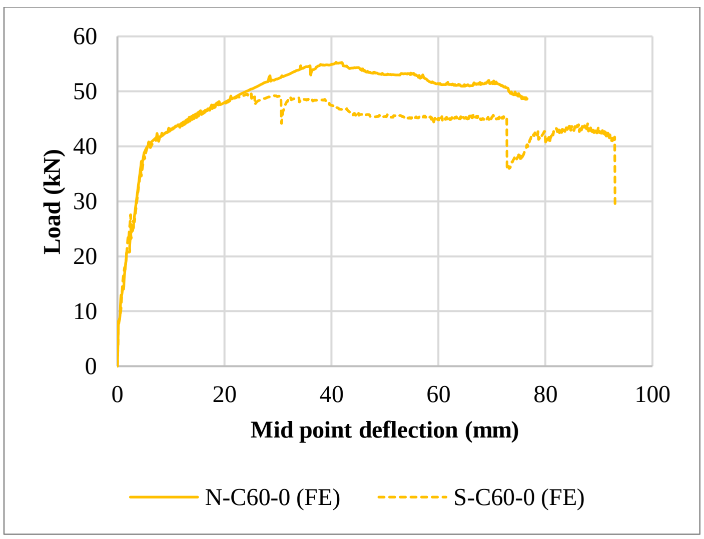

(a)

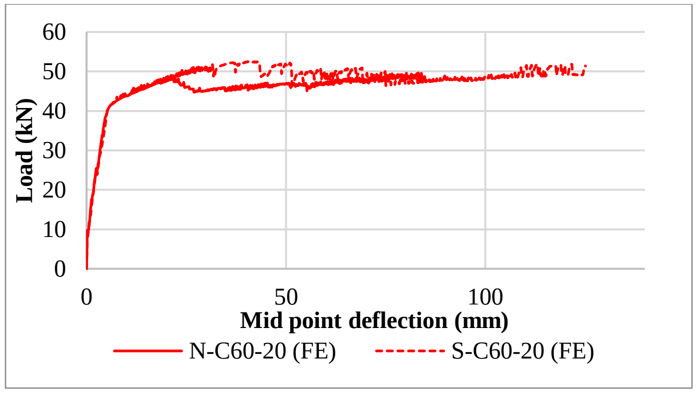

(b)

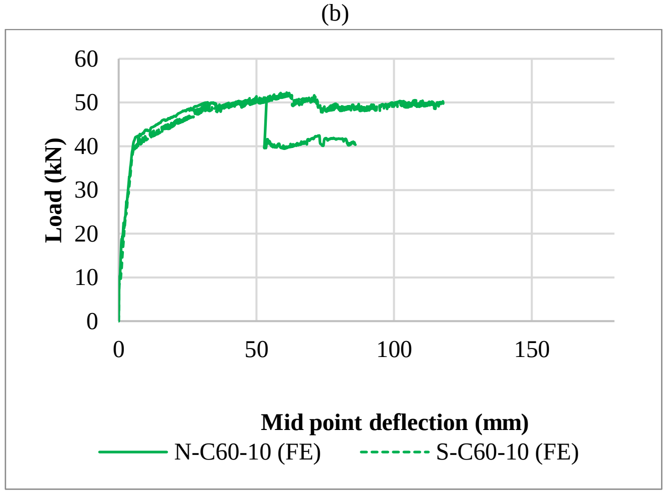

(c)

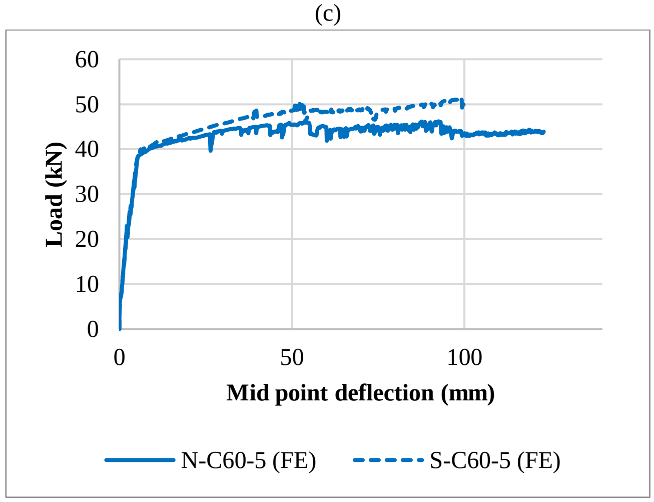

(d)

Figure 10. Load-displacement graphs for the variation in concrete type (a) 0 cm, (b) 20 cm, (c) 10 cm, (d) 5 cm.

When all the graphs in Figure 11 are analyzed, it can be seen that the energy consumption capacity of the elements produced using SCC is the same or about 25% less than the elements produced using NC. The highest energy was consumed by N-C60-10 with an energy value of 7.46 kN.

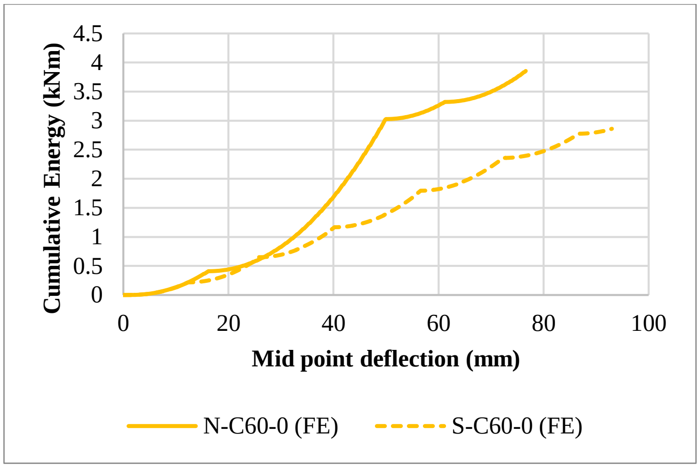
Cumulative Energy (kNm)
4.5
4
3.5
3
2.5
2
1.5
1
0.5
0
0
20
40
60
80
100
Mid point deflection (mm)
N-C60-0 (FE)
S-C60-0 (FE)

(a)

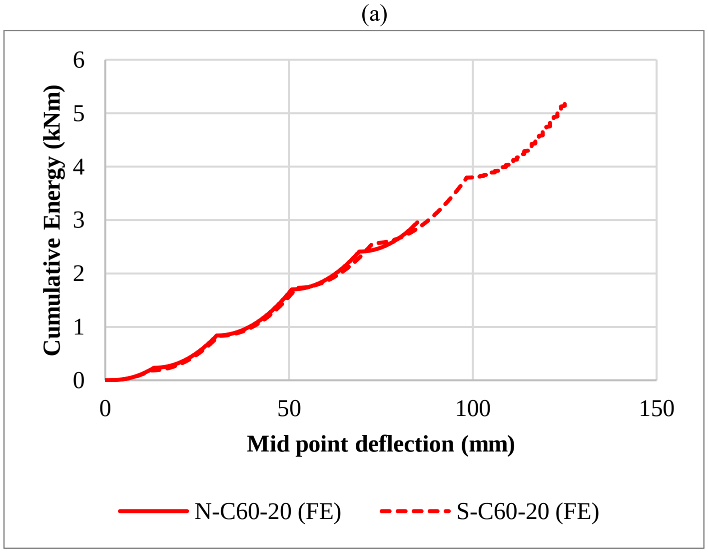
Cumulative Energy (kNm)
6
5
4
3
2
1
0
0
50
100
150
Mid point deflection (mm)
N-C60-20 (FE)
S-C60-20 (FE)

(b)

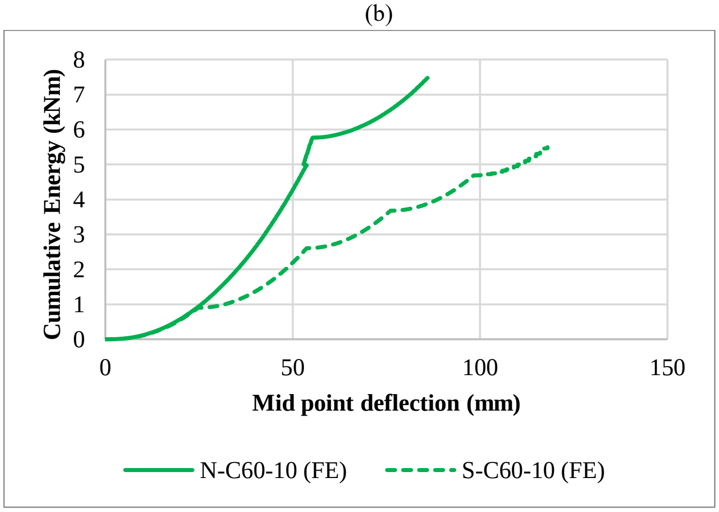
Cumulative Energy (kNm)
8
7
6
5
4
3
2
1
0
0
50
100
150
Mid point deflection (mm)
N-C60-10 (FE)
S-C60-10 (FE)

(c)

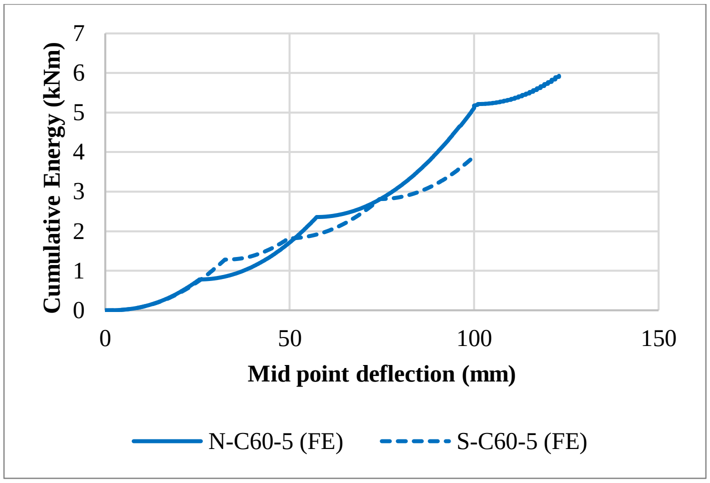

(d)

Figure 11. Energy consumption graphs for the variation in concrete type (a) 0 cm, (b) 20 cm, (c) 10 cm, (d) 5 cm.

3.3. Effect of concrete strength

To investigate the effect of concrete strength on the behavior of reinforced concrete beams, SCC beams designed with the same stirrup spacing were compared. Load-displacement graphs for the change in concrete strength are shown in Figure 12. The beams designed in both concrete strengths have similar load carrying capacities. The maximum displacement value is 150 mm for specimen S-30-5. The minimum displacement was observed for S-C60-0.

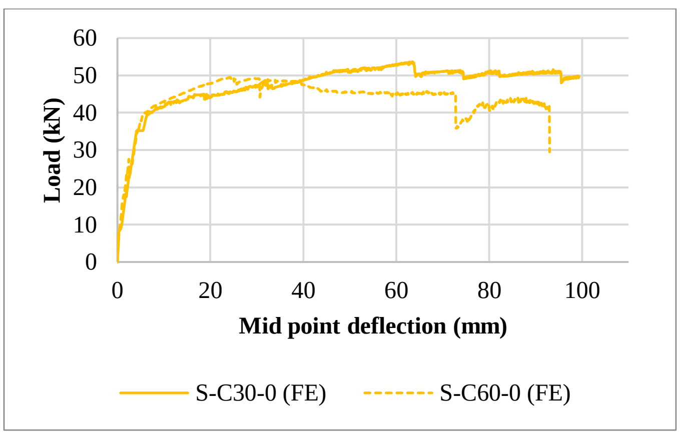

(a)

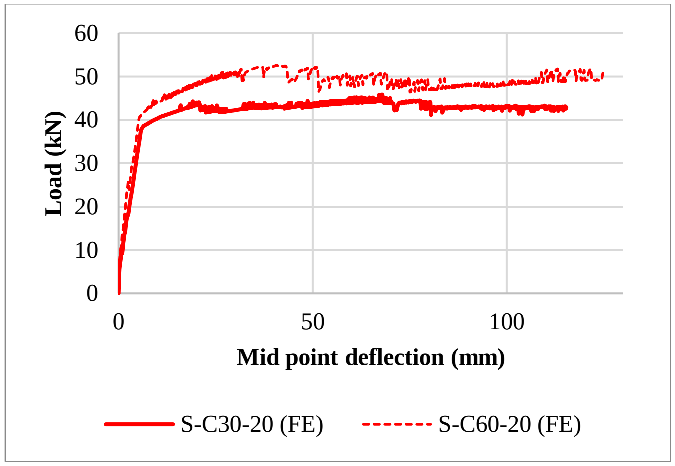

(b)

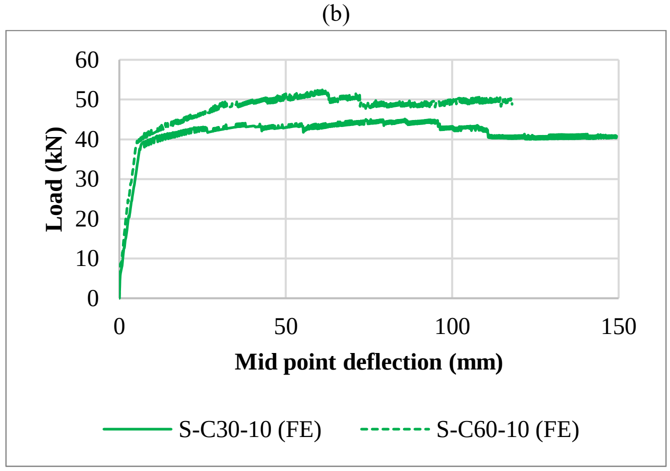

(c)

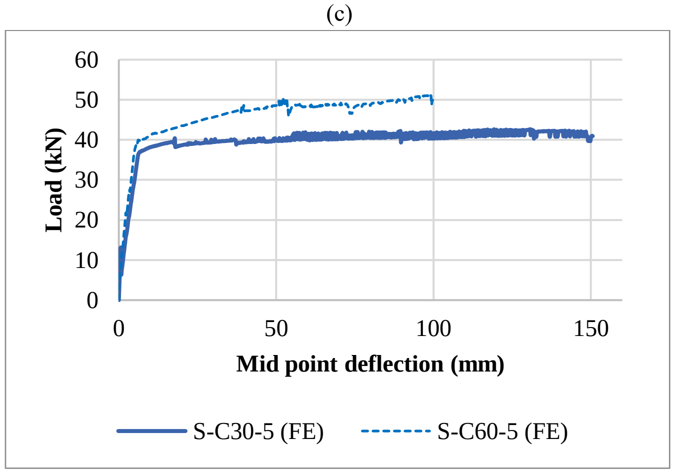

(d)

Figure 12. Load-displacement graphs for the change in concrete strength (a) 0 cm, (b) 20 cm, (c) 10 cm, (d) 5 cm.

When the energy graphs for the change in concrete strength are analyzed, it is seen that the energy consumption capacity of SCC beams with C30 strength is higher than that of beams with C60 strength (Figure 13). S-C30 beams with 5 cm and 10 cm stirrup spacing consumed approximately the same amount of energy as S-C60 beams with the same stirrup spacing. Although the cumulative energy consumption was approximately the same for specimens with 5 cm and 20 cm stirrups, the energy consumption of S-C60 specimens at yield was higher than that of S-C30 specimens.

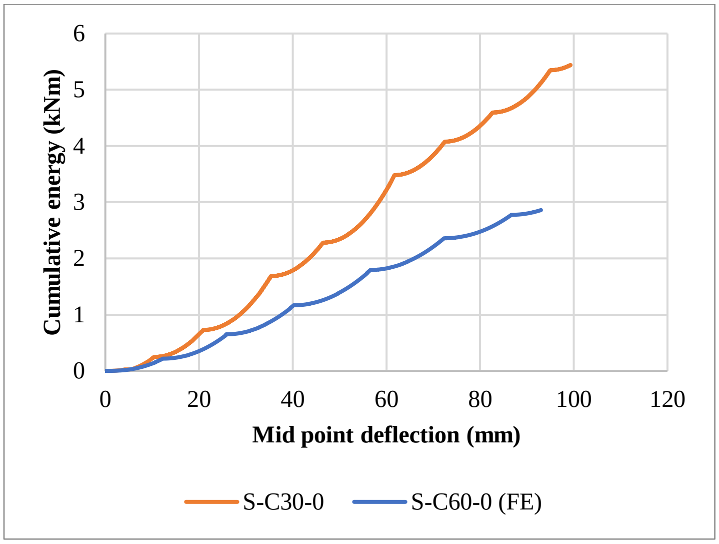
Cumulative energy (kNm)
Mid point deflection (mm)
S-C30-0
S-C60-0 (FE)

(a)

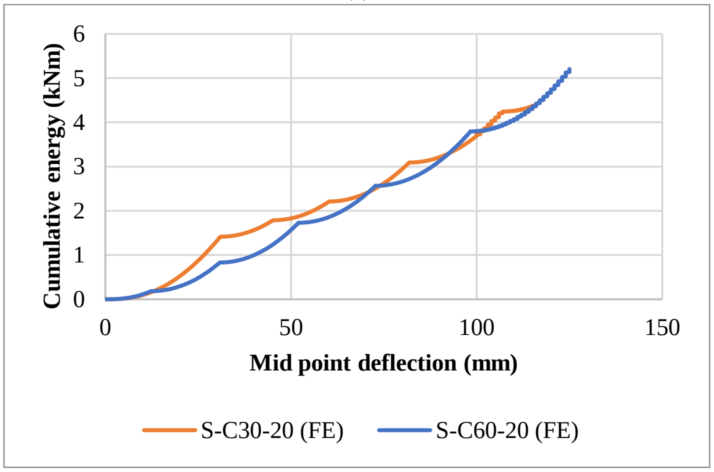
Cumulative energy (kNm)
Mid point deflection (mm)
S-C30-20 (FE)
S-C60-20 (FE)

(b)

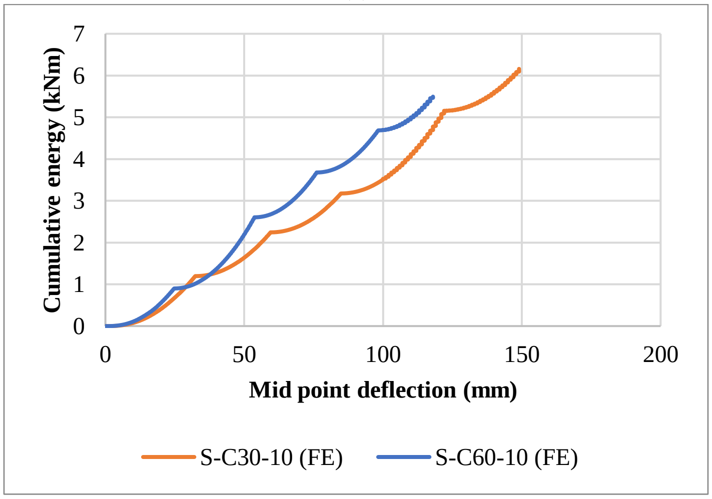
Cumulative energy (kNm)
Mid point deflection (mm)
S-C30-10 (FE)
S-C60-10 (FE)

(c)

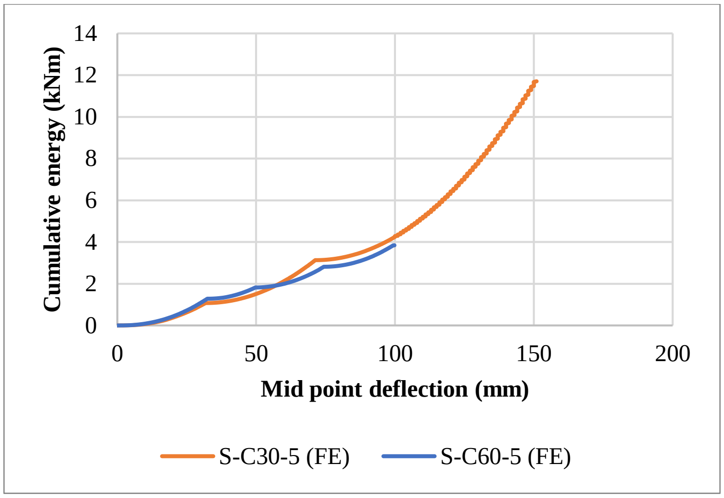

(d)

Figure 13. Energy consumption graphs of group 3 (a) 0 cm, (b) 20 cm, (c) 10 cm, (d) 5 cm.

The data obtained from the test was given in Table 6. When the table is examined, N-C60-0 has 41.91 kN load at the yield point. However, the most displaced element was S-C30-5 with a displacement value of 150.6 mm, while the least displaced element was N-C60-0 with a displacement value of 76.47 mm. On the other hand, the experimental study results are examined, the specimen with the highest load bearing capacity is N-C60-5 with a value of 51.48 kN. However, the highest displaced element was S-C30-5 with a displacement value of 160.3 mm, while the lowest displaced was N-C60-0 with a displacement value of 70.22 mm. The ductility rates obtained by taking the ratio of fracture to yield displacement in the test specimens are shown in Table 6. All test members reached the yield point and all specimens showed flexural behavior up to this point. It can be seen that the ductility of the specimens without stirrups and with small stirrup spacing is particularly low compared to the other specimens. In addition, the ductility of SCC specimens is higher than NC specimens.

Table 6. Analysis results of all specimens.

Specimen	Load capacity (kN)		Deflection (mm)		Ductility ratio	Yield stiffness (kN/mm)
	Yield	Failure	At Yield	At failure		
N-C30-0	37.11	43.71	6.94	93.55	13.48	5.34
N-C30-20	37.52	40.76	6.92	134.76	19.47	5.42
N-C30-10	37.71	40.33	5.98	149.30	24.96	6,30
N-C30-5	37.88	50.10	5.67	88.74	15.65	6.68
S-C30-0	39.53	51.06	6.37	82.00	12.87	6.20
S-C30-20	38.43	42.58	6.30	115.27	18.29	6.10
S-C30-10	38.97	40.34	6.79	149.28	21.98	5.74
S-C30-5	36.56	40.93	7.53	150.6	20.00	4.85
N-C60-0	40.06	48.56	6.10	76.47	12.53	6.56
N-C60-20	40.68	47.78	6.05	84.90	14.03	6.72
N-C60-10	41.91	40.35	6.64	85.95	12.94	6.31
N-C60-5	37.99	43.89	5.31	123.01	23.16	7.15
S-C60-0	39.78	41.06	6.13	92.74	15.13	6.49
S-C60-20	40.49	49.15	5.34	124.45	23.30	7.58
S-C60-10	39.18	48.80	5.59	117.98	21.10	6.83
S-C60-5	39.84	48.77	6.42	99.36	15.47	6.20

3.4. Comparison of experimental and numerical results

All the numerical results obtained in the study were compared with the results of the experimental study. When the damage conditions and failure modes of the elements were analyzed, it was found that the stresses and damage in all the elements were similar to the damage conditions in the experimental study. As an example, Figure 14 shows the damage conditions of the element with 10 cm stirrup spacing and C30 concrete strength made with normal concrete.

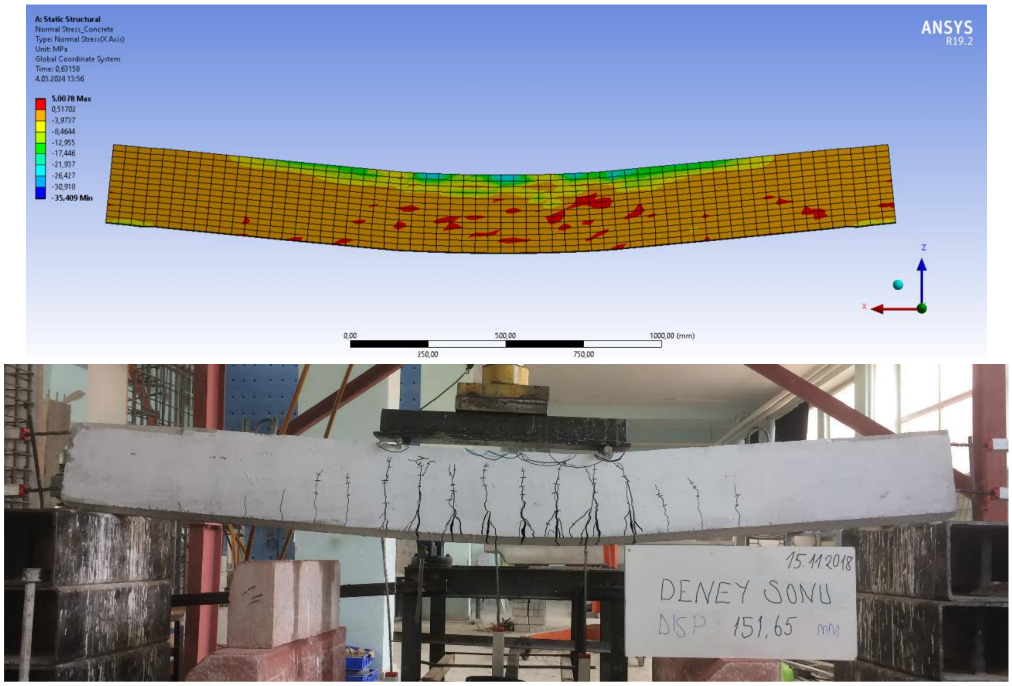

Figure 14. Experimental and numerical analysis comparison of specimen N-C30-10.

The load displacement curves obtained from the numerical study were compared with the load displacement curves obtained from the experimental study. The reinforced concrete behavior in the numerical study was found to be consistent with the experimental study. When the general appearance of the load-displacement graphs is analyzed, it is seen that the results are consistent with each other (Figure 15).

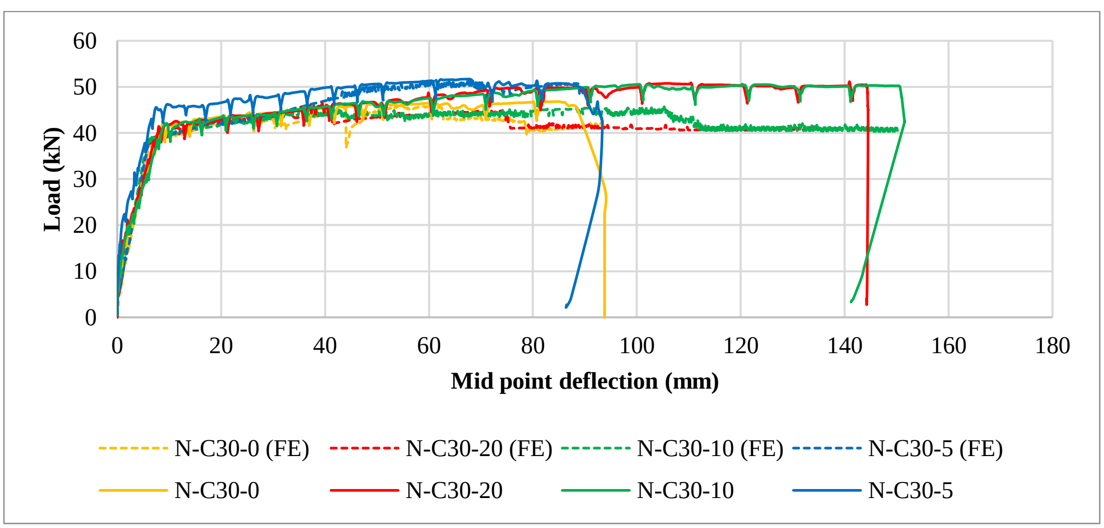

(a)

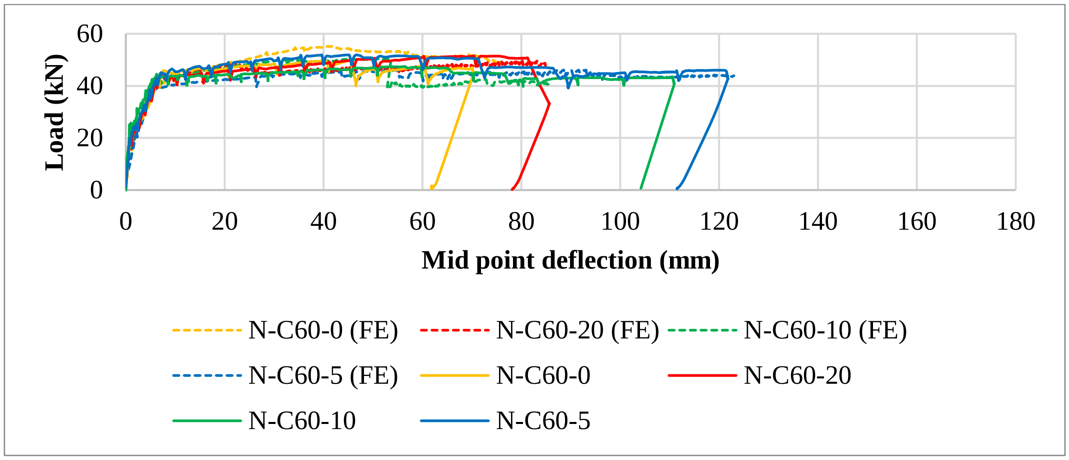

(b)

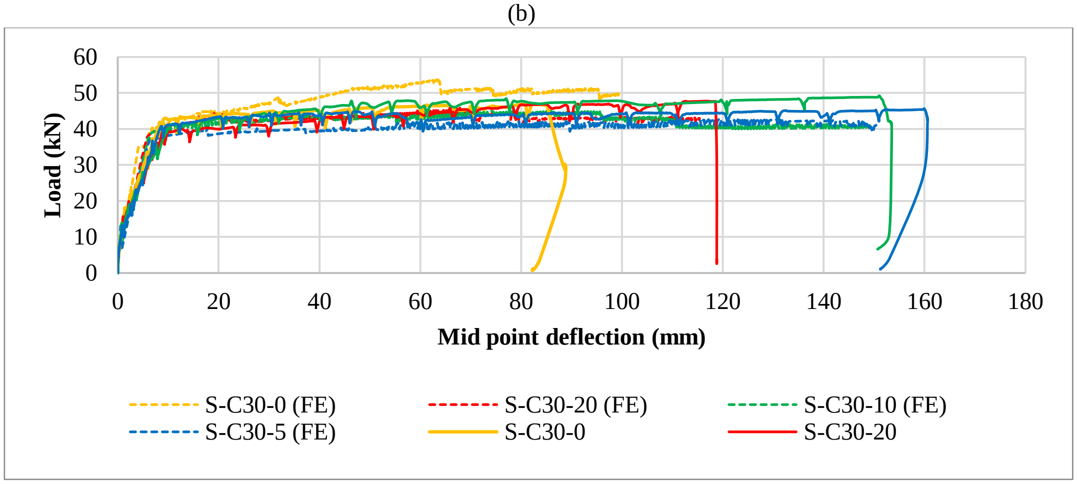

(c)

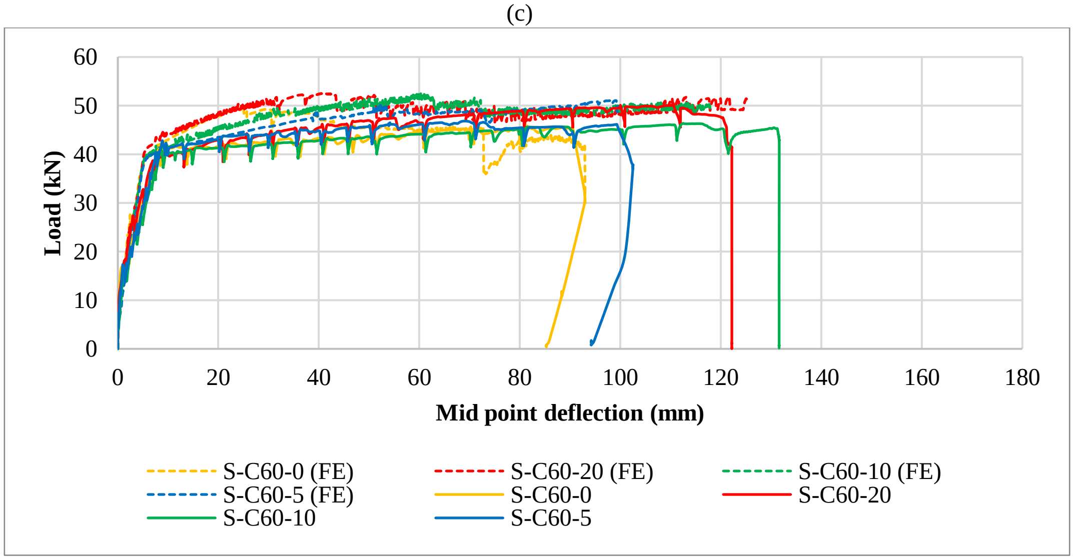

(d)

Figure 15. Experimental and numerical comparison of load-displacement curves of specimens, (a) N-C30, (b) S-C30, (c) N-C60, (d) S-C60.

In the numerical study, the largest deviation with respect to the yield load was 11.66% and this deviation occurred in the N-C30-0 specimen. In terms of maximum load carrying capacity, the largest deflections were observed in specimens without stirrups. When the deflection with respect to the ultimate displacement was analyzed, the largest deflection of 10.64% was observed in specimen N-C60-10. Also, the maximum load carrying capacity and maximum displacement of all specimens are given in Table 7.

Table 7. Comparison of results.

Specimen	Analysis results				Experimental results			
	Load capacity (kN)		Deflection (mm)		Load capacity (kN)		Deflection (mm)	
	Yield	Failure	Yield	Failure	Yield	Failure	Yield	Failure
N-C30-0	37.11	43.71	6.94	93.55	41.44	44.93	8.81	88.66
N-C30-20	37.52	40.76	6.92	134.76	37.89	45.28	7.51	144.22
N-C30-10	37.71	40.33	5.98	149.30	38.92	42.34	8.30	151.53
N-C30-5	37.88	50.10	5.67	88.74	41.73	49.57	6.76	89.66
S-C30-0	39.53	51.06	6.37	82.00	38.61	46.39	7.63	85.19
S-C30-20	38.43	42.58	6.30	115.27	38.60	43.85	8.95	111.12
S-C30-10	38.97	40.34	6.79	149.28	35.27	41.56	8.50	151.61
S-C30-5	36.56	40.93	7.53	150.6	37.76	42.58	8.97	160.60
N-C60-0	40.06	48.56	6.10	76.47	42.96	46.26	6.83	70.15
N-C60-20	40.68	47.78	6.05	84.90	41.71	50.75	6.61	81.27
N-C60-10	41.91	40.35	6.64	85.95	42.54	41.00	5.34	77.68
N-C60-5	37.99	43.89	5.31	123.01	39.43	42.93	5.39	121.77
S-C60-0	39.78	41.06	6.13	92.74	39.40	44.77	7.71	90.65
S-C60-20	40.49	49.15	5.34	124.45	37.91	46.89	7.36	120.63
S-C60-10	39.18	48.80	5.59	117.98	38.67	45.02	8.97	131.31
S-C60-5	39.84	48.77	6.42	99.36	40.01	45.32	8.18	99.60

4. Conclusions and comments

Within the scope of the study, 16 reinforced concrete beams were numerically analyzed in 4-point bending mechanism. In the analyses, the flexural behavior of SCC beams and the effect of stirrup ratio and concrete class on the behavior were investigated. Load carrying capacities, ductility ratios, energy consumption capacities, stiffness and load-displacement curves of the beams were analyzed. The following results were obtained from the data obtained.

1. Load values at the first crack are lower for SCC beams than NC beams. The maximum load values of SCC beams are also lower than those of NC beams. The load carrying capacity of NC beams is higher because the amount of coarse aggregate in NC beams is higher than the amount of coarse aggregate in SCC beams. The aggregate size in SCC is smaller than in NC. Therefore, the less interfacial transition zone caused the strength of NC to be higher than that of SC.
2. The numerical analyses performed with ANSYS software are consistent with the results of the experimental study.
3. The tensile reinforcement in all specimens reached the yield point at an average load of 42 kN. The displacement values at the same point also gave approximate results.
4. The initial stiffness of the NC beams was much higher than that of the SCC beams. This shows that NC is more rigid than SCC.
5. The beams produced with SCC consumed similar amounts of energy as those produced with NC.
6. As a result of the analyses, in general, as the stirrup spacing decreases, the beams are displaced more and as a result, the energy consumed and the element ductility increase. In this respect, stirrup spacing in beams is decisive for the behavior of beams.
7. In the light of all these analyses, it is seen that the beams produced with SCC are close to NC beams in terms of load carrying capacity and stiffness.

8. The use of sufficient shear reinforcement in beams improves beam behavior. As a result of the experimental study, it was concluded that over or under use of shear reinforcement in beams adversely affects the beam behavior.
9. SCC is a more durable concrete than NC. Although they show mechanically similar behavior, it is predicted that the behavior of SCC and NC elements under different physical conditions will be different. Therefore, it would be appropriate for future studies to examine the behavior of SCC and NC elements subjected to environmental effects such as sulfate effect, freeze-thaw effect.

Author contributions: Salih Cengiz: Methodology, Conceptualization, Resources, Investigation, Experimental Study, Analyzing, Writing, -review & editing, Supervision.
Abdulkadir Solak: Methodology, Conceptualization, Resources, Modelling, Analyzing, Writing, -review & editing, Supervision.
Alptuğ Ünal: Methodology, Conceptualization, Resources, Experimental Study, Analyzing, Writing, -review & editing, Supervision.
Mehmet Kamanlı: Methodology, Conceptualization, Resources, Experimental Study, Analyzing, review & editing, Supervision.

Funding: This study was funded by Konya Technical University Coordinating Office.

Acknowledgments: The authors would like to thank the Scientific Research Projects (KTUN-BAP-18201111-Konya, Turkey) of Konya Technical University Coordinating Office for financial support. This study was prepared from master thesis of Salih Cengiz with the advisor of Mehmet Kamanli.

Conflicts of interest: There are no conflicts of interest.

References

Abd, S. M., Mhaimeed, I. S., Tayeh, B. A., Najm, H. M., Qaidi, S. (2023). Investigation of the use of textile carbon yarns as sustainable shear reinforcement in concrete beams. Case Studies in Construction Materials, 18, 1-13. https://doi.org/10.1016/j.cscm.2022.e01765

Ahmad, S., Umar, A., & Masood, A. (2017). Properties of normal concrete, self-compacting concrete and glass fibre-reinforced self-compacting concrete: an experimental study. Procedia engineering, 173, 807-813. https://doi.org/https://doi.org/10.1016/j.proeng.2016.12.106

Akça, K. R., İpek, M., Çelenk, S., & Karabulak, A. (2023). Experimental investigation on mechanical properties of HSSCC containing waste steel fibers obtained from end-of-life tires. Revista De La Construcción. Journal of Construction, 22(1), 87–101. https://doi.org/10.7764/RDLC.22.1.8

Akinpelu, M. A., Odeyemi, S. O., Olafusi, O. S., & Muhammed, F. Z. (2017). Evaluation of splitting tensile and compressive strength relationship of self-compacting concrete. Journal of King Saud University-Engineering Sciences. https://doi.org/https://doi.org/10.1016/j.jksues.2017.01.002

Alabdulkarim, A., El-Sayed, A. K., Alsaif, A. S., Fares, G., & Alhozaimy, A. M. (2024). Behavior of Lightweight Self-Compacting Concrete with Recycled Tire Steel Fibers. Buildings, 14(8), 2463. https://doi.org/10.3390/buildings14082463

Alam, M., & Hussein, A. (2017). Relationship between the shear capacity and the flexural cracking load of FRP reinforced concrete beams. Construction and Building Materials, 154, 819-828. https://doi.org/https://doi.org/10.1016/j.conbuildmat.2017.08.006

Alexandra, C., Bogdan, H., Camelia, N., & Zoltan, K. (2018). Mix design of self-compacting concrete with limestone filler versus fly ash addition. Procedia Manufacturing, 22, 301-308. https://doi.org/https://doi.org/10.1016/j.promfg.2018.03.046

Alhadid, M. M. A., & Youssef, M. A. (2017). Analysis of reinforced concrete beams strengthened using concrete jackets. Engineering Structures, 132, 172-187. https://doi.org/Analysis of reinforced concrete beams strengthened using concrete jackets.

Altın, M., Cogurcu, M. T., & Donduren, M. S. (2006). Kendiliğinden yerleşen betonun dayanim özellikleri için deneysel bir çalışma. Selçuk-Teknik Dergisi, 5(3), 77-88. http://sutod.selcuk.edu.tr/sutod/article/view/27

Alyousif, A., Anil, O., Sahmaran, M., Lachemi, M., Yildirim, G., & Ashour, A. F. (2015). Comparison of shear behaviour of engineered cementitious composite and normal concrete beams with different shear span lengths. Magazine of Concrete Research, 68(5), 217-228. https://doi.org/https://doi.org/10.1680/jmacr.14.00336

ANSYS User's Guide. (2018). Ansys, Release 19.2. Part IV Legacy Elements, Solid65 Element Description, ANSYS, Inc.

Aydın, A. C., & Bayrak, B. (2016). Kendiliğinden yerleşen ve normal betonlu betonarme kirişlerin burulma davranışının deneysel incelenmesi. Sinop Üniversitesi Fen Bilimleri Dergisi, 1(1), 23-32. https://dergipark.org.tr/tr/pub/sinopfbd/issue/23605/234961

Benaicha, M., Alaoui, A. H., Jalbaud, O., & Burtschell, Y. (2019). Dosage effect of superplasticizer on self-compacting concrete: correlation between rheology and strength. Journal of Materials Research and Technology, 8(2), 2063-2069. https://doi.org/https://doi.org/10.1016/j.jmrt.2019.01.015

Cengiz, S. (2019). Investigation of Shear and Flexural Behavior of Constant Rectangular Sectioned Reinforced Concrete Beams Produced with Self Compacting Concrete [MS., Konya Technical University]. Konya.

Cengiz, S., Kamanli, M., & Unal, A. (2020). Investigation of flexural behavior of reinforced concrete beams produced with self compacting and normal concrete. 8(2), 429-438. https://doi.org/https://doi.org/10.21923/jesd.672314

Cladera, A., & Mari, A. (2005). Experimental study on high-strength concrete beams failing in shear. Engineering Structures, 27(10), 1519-1527. https://doi.org/https://doi.org/10.1016/j.engstruct.2005.04.010

Ebead, U. (2015). Inexpensive strengthening technique for partially loaded reinforced concrete beams: Experimental study. Journal of materials in civil engineering, 27(10), 04015002. https://doi.org/https://doi.org/10.1061/(ASCE)MT.1943-5533.0001249

El-Sayed, A. K. (2017). Shear capacity assessment of reinforced concrete beams with corroded stirrups. Construction and Building Materials, 134, 176-184. https://doi.org/https://doi.org/10.1016/j.aej.2018.03.012

El Zareef, M. A., & El Madawy, M. E. (2018). Effect of glass-fiber rods on the ductile behaviour of reinforced concrete beams. Alexandria engineering journal, 57(4), 4071-4079. https://doi.org/https://doi.org/10.1016/j.aej.2018.03.012

Fiol, F., Thomas, C., Muñoz, C., Ortega-López, V., & Manso, J. (2018). The influence of recycled aggregates from precast elements on the mechanical properties of structural self-compacting concrete. Construction and Building Materials, 182, 309-323. https://doi.org/https://doi.org/10.1016/j.conbuildmat.2018.06.132

Hemzah, S. A., Alyhya, W. S., & Hassan, S. A. (2020). Experimental investigation for structural behaviour of self-compacting reinforced concrete hollow beams with in-place circular openings strengthened with CFRP laminates. Structures, 24, 99-106. https://doi.org/10.1016/j.istruc.2020.01.008

Hognestad, E. (1951). Study of combined bending and axial load in reinforced concrete members. University of Illinois at Urbana Champaign, College of Engineering URL: http://hdl.handle.net/2142/4360

Hosseinimehrab, E., Sadeghi, A., & Farsangi, E. N. (2021). Finite Element Modeling of Self-Compacting Concrete Beams Under Shear. Civil and Environmental Engineering Reports, 31(4), 1-16.

Jiang, C.-J., Yu, J.-T., Li, L.-Z., Wang, X., Wang, L., & Liao, J.-H. (2018). Experimental study on the residual shear capacity of fire-damaged reinforced concrete frame beams and cantilevers. Fire Safety Journal, 100, 140-156. https://doi.org/https://doi.org/10.1016/j.firesaf.2018.08.004

Jindal, A., Ransinchung, G., & Kumar, P. (2019). Behavioral study of self-compacting concrete with wollastonite microfiber as part replacement of sand for pavement quality concrete (PQC). International Journal of Transportation Science and Technology. https://doi.org/https://doi.org/10.1016/j.ijtst.2019.06.002

Kaltakci, M. Y., & Kamanli, M. (2001). An Experimental Study on Behaviour of Variable I Sectioned Beams under Flexure Produced by Normal and Lightweight Concrete. 30. https://doi.org/10.2495/CMEM010391

Kamal, M., Safan, M., Bashandy, A., & Khalil, A. (2018). Experimental investigation on the behavior of normal strength and high strength self-curing self-compacting concrete. Journal of Building Engineering, 16, 79-93. https://doi.org/https://doi.org/10.1016/j.jobe.2017.12.012

Kamanlı, M. (1999). Theoretical and Experimental Investigations on Beams with Variable Cross-Section [PhD., Selcuk University]. Konya.

Kamanli, M., & Unal, A. (2018). Investigation of shear behavior of reinforced concrete beams under simple and fixed support conditions. Selçuk Üniversitesi Mühendislik, Bilim Ve Teknoloji Dergisi, 6(2), 218-226. https://doi.org/https://doi.org/10.15317/Scitech.2018.128

Khan, S. U., & Ayub, T. (2020). Flexure and shear behaviour of self-compacting reinforced concrete beams with polyethylene terephthalate fibres and strips. Structures, 25, 200-211. https://doi.org/10.1016/j.istruc.2020.02.023

Kodur, V., Solhmirzaei, R., Agrawal, A., Aziz, E. M., & Soroushian, P. (2018). Analysis of flexural and shear resistance of ultra high-performance fiber reinforced concrete beams without stirrups. Engineering Structures, 174, 873-884. https://doi.org/https://doi.org/10.1016/j.engstruct.2018.08.010

Mahmod, M., Hanoon, A. N., & Abed, H. J. (2018). Flexural behavior of self-compacting concrete beams strengthened with steel fiber reinforcement. Journal of Building Engineering, 16, 228-237. https://doi.org/10.1016/j.jobe.2018.01.006

Mohammed, A. A. (2017). Flexural behavior and analysis of reinforced concrete beams made of recycled PET waste concrete. Construction and Building Materials, 155, 593-604. https://doi.org/https://doi.org/10.1016/j.conbuildmat.2017.08.096

Niewiadomski, P., Hoła, J., & Ćwirzeń, A. (2018). Study on properties of self-compacting concrete modified with nanoparticles. Archives of Civil and Mechanical Engineering, 18(3), 877-886. https://doi.org/10.1016/j.acme.2018.01.006

Okamura, H. (1997). Self-compacting high-performance concrete. Concrete international, 19(7), 50-54.

Okamura, H., & Ouchi, M. (1999). Self-Compacting Concrete Development, Present and Future 1st International Rilem Symposium on Self Compacting Concrete, Sweden.

Özkılıç, Y. O., Karalar, M., Aksoylu, C., Beskoplylny, A. N., Stel'makh S. A., Shcherban, E. M., Qaidi, S., Pereira, I. S. A., Monteiro, S. N., Azevedo, A, R, G. (2023). Shear performance of reinforced expansive concrete beams utilizing aluminium waste. Journal of Materials Research and Technology, 24, 5433-5448. https://doi.org/10.1016/j.jmrt.2023.04.120

Pająk, M. (2016). Investigation on flexural properties of hybrid fibre reinforced self-compacting concrete. Procedia engineering, 161, 121-126. https://doi.org/10.1016/j.proeng.2016.08.508

Pająk, M., & Ponikiewski, T. (2017). Experimental investigation on hybrid steel fibers reinforced self-compacting concrete under flexure. Procedia engineering, 193, 218-225. https://doi.org/https://doi.org/10.1016/j.proeng.2017.06.207

Pawłowski, D., & Szumigała, M. (2015). Flexural behaviour of full-scale basalt FRP RC beams–experimental and numerical studies. Procedia engineering, 108, 518-525. https://doi.org/https://doi.org/10.1016/j.proeng.2015.06.114

Qeshta, I. M., ShaFigh, P., & Jumaat, M. Z. (2015). Flexural behaviour of RC beams strengthened with wire mesh-epoxy composite. Construction and Building Materials, 79, 104-114. https://doi.org/https://doi.org/10.1016/j.conbuildmat.2015.01.013

Rahal, K., & Alrefaei, Y. (2018). Shear strength of recycled aggregate concrete beams containing stirrups. Construction and Building Materials, 191, 866-876. https://doi.org/https://doi.org/10.1016/j.conbuildmat.2018.10.023

Shatarat, N., Mahmoud, H. M., & Katkhuda, H. (2018). Shear capacity investigation of self-compacting concrete beams with rectangular spiral reinforcement. Construction and Building Materials, 189, 640-648. https://doi.org/https://doi.org/10.1016/j.conbuildmat.2018.09.046

Sin, L. H., Huan, W. T., Islam, M. R., & Mansur, M. A. (2011). Reinforced Lightweight Concrete Beams in Flexure. ACI Structural Journal, 108(1). http://worldcat.org/oclc/13846957

Topçu, İ. B., Bilir, T., & Baylavli, H. (2008). Kendiliğinden Yerleşen Betonun Özellikleri. Eskişehir Osmangazi Üniversitesi Mühendislik ve Mimarlık Fakültesi Dergisi, 21(1s), 1-22.

Turkish Building Earthquake Code, TBEC (2018)., Deprem Etkisi Altında Binaların Tasarımı için Esaslar, Afet ve Acil Durum Yönetimi Başkanlığı, Ankara

Uğur, A. E., Ünal A. (2022). Assessing the structural behavior of reinforced concrete beams produced with macro synthetic fiber reinforced self-compacting concrete, Structures, Volume 38, Pages 1226-1243, https://doi.org/10.1016/j.istruc.2022.02.051.

Unal, A., Kamanli, M., & Cengiz, S. (2018). Effect of Stirrup Ratio on the Shear Behavior of 1/2 Scale RC Beams. Int. J. Struct. Civ. Eng. Res. https://doi.org/10.18178/ijscer.7.4.309-313

Ünal, A., Kamanlı, M., Solak, A., Cengiz, S., 2023, Numerical investigation of the effect of support conditions on beam shear behaviour in full scale reinforced concrete beams, GRAĐEVINAR, 75/12 1193-1201.

Willam, K. J. (1974). Constitutive model for the triaxial behavior of concrete. IABSE Seminar on Concrete Structure subjected Triaxial Stresses, 1-30

Yang, Y., Xue, Y., Yu, Y., Ma, N., & Shao, Y. (2017). Experimental study on flexural performance of partially precast steel reinforced concrete beams. Journal of Constructional Steel Research, 133, 192-201. https://doi.org/10.1016/j.jcsr.2017.02.019

Yousef, A. M., Tahwia, A. M., & Marami, N. A. (2018). Minimum shear reinforcement for ultra-high-performance fiber reinforced concrete deep beams. Construction and Building Materials, 184, 177-185. https://doi.org/https://doi.org/10.1016/j.conbuildmat.2018.06.022

Yuan, Y., & Wang, Z. (2019). Shear behavior of large-scale concrete beams reinforced with CFRP bars and handmade strip stirrups. Composite Structures, 111253. https://doi.org/https://doi.org/10.1016/j.compstruct.2019.111253